Indian Journal of Pure & Applied Physics
Vol. 52, July 2014, pp. 491-498

Structural and optical properties of vanadium doped akaline earth lead zinc phosphate glasses

S Sreehari Sastry[1]* & B Rupa Venkateswara Rao[1,2]

[1]Department of Physics, Acharya Nagarjuna University, Nagarjunanagar 522 510, India

[2]Department of Physics,V R Siddhartha Engineering College, Vijayawada 520 007, India

*E-mail: sreeharisastry@yahoo.com

Received 7 January 2014; revised 18 April 2014; accepted 20 May 2014

The structural properties of vanadium doped alkaline earth lead zinc phosphate glasses have been investigated by XRD, UV-Visible, EPR, FT-IR and Raman spectroscopy techniques. XRD analysis has confirmed that the samples are X-ray amorphous. The optical band gap energy (E_{opt}) is observed to decrease with the replacement of alkaline earth content, whereas reverse trend is observed in Urbach energy (ΔE) and optical basicity (Λ_{th}). The spin-Hamiltonian parameter, dipolar hyperfine coupling and covalency parameters have been obtained from EPR spectra. Depolymerization of the phosphate network by the replacement of alkaline earth content in glasses which are consisting of mainly PO_3^{2-} and PO_4^{3-} units, was detected by FT-IR spectra. The structural modification due to breakage of P=O bond and the formationof P–O–P bonds in the different compositions have been studied by Raman spectra. The physical properties have been measured and observed to increase with the replacement of alkaline earth content. The replacement of BaO has improved the strength of the cross-links between the phosphate chains of the glass.

Keywords: Phosphate glass, Optical absorption, EPR, FT-IR, Raman spectra, Tauc's plot

1 Introduction

Phosphate glass is a special optical glass that is formed with the network of P_2O_5. Electronically phosphate glasses often have larger band gaps than silicates and, therefore, act as a better ultraviolet (UV) transmission[1]. Phosphate glasses also have low dispersion and relatively high refractive indices and are developed for achromatic optical elements. These glasses have high ionic conductivity as well as thermal and electrochemical stability. Therefore, these glasses are extensively studied for many technological applications such as solid-state ionic devices, photonic materials and biomedical materials[2-4].

The addition of transition metal (TM) oxides like V_2O_5 to P_2O_5 glasses, in general, offers the possibility to exhibit both semiconducting[5], and magnetic properties which will lead to a deploymerization of the network, by breaking of P-O-P linkages and generation[6] of NBO's. Wazer[7] suggested that with the addition of transition metal oxide, the degradation rate of phosphate glass can be reduced significantly. V_2O_5 have very high potentiality in the application use like optoelectronic devices and electrochromic display device[8] (EDD). Interpretation of structural aspects and physical-chemical properties of alkaline earth phosphate glasses is to be made only after accounting the moisture contents in the glasses. Though the development and technological applications of phosphate glasses have been limited initially by their poor chemical durability, the problem of durability eventually being solved by the inclusion of suitable intermediates like MgO, CaO, SrO and BaO. Electron paramagnetic resonance (EPR) studies are important and useful techniques in understanding the microscopic properties in glasses[9]. Infrared and Raman spectroscopic studies for vitreous P_2O_5, are useful to distinguish bridging and terminal oxygen atoms[10,11]. Therefore, in the present paper an attempt is made to report on EPR, optical absorption, IR and Raman studies on vanadium doped alkaline earth lead zinc phosphate glasses containing alkaline earth oxides (MgO, CaO, SrO and BaO).

2 Experimental Details

Primarily the materials used in the study are of the analytical grade phosphorus pentoxide (P_2O_5) (99.9% pure), lead oxide (Pb_3O_4), zinc oxide (ZnO), 0.1 mole% of vanadium pentoxide (V_2O_5), magnesium oxide (MgO), calcium oxide (CaO), strontium oxide (SrO), barium oxide (BaO) which are added as an intermediate compound to each glass composition. These materials are weighed to get the

required composition and grounded in a mortar with pestle for half an hour to obtain homogeneous mixtures. Each sample is being melted in a porcelain crucible in an electric furnace at 950°C for about one hour. The homogeneous melt is rapidly quenched on to a stainless steel plate by maintaining constant temperature of 370°C. The glasses are annealed for 5 h at 370°C for relieving mechanical stresses, if any.

The X-ray diffractograms (XRD) are recorded on powder samples of all the glass samples at room temperature using a Philips X-ray generator (Model PW1170) with CuKα radiation (λ=1. 5418 Å) in the 2Θ ranges 10°-70° at a scanning rate of 2° per min. The optical absorption spectra of these glasses are recorded with a resolution of 0.1 nm at room temperature using UV-Vis-NIR spectrophotometer (JASCO model V-670 UV-Vis-NIR) in the wavelength region 200-900 nm. EPR spectra of the samples are recorded at room temperature through a BRUKER-ER073 series EPR spectrometer operating in the X-band frequency (9.4 GHz) with 100 kHz field modulation. The magnetic field is scanned from 0 to 800 mT and the microwave power of 1mW is used. The infrared spectra of these glasses are recorded on SHIMADZU 8201 PC FT-IR Spectrophotometer in the range 400-4000 cm^{-1} using KBr pellets. The fine glass powder is examined by using Fourier Transform Raman spectrometer (model BRUKER RFS 27: Standalone FT-Raman Spectrometer) equipped with Nd:YAG laser 1064 nm, which has the property of eliminating the problem of sample fluorescence and photo-decomposition. The Raman spectra are recorded with the 0.7 W laser power, 64 scans and 2 cm^{-1} resolution. The spectra of the samples are measured in the range 200-3700 cm^{-1}. The procedures and formulae used here to determine the physical properties are similar in nature as in earlier works[12].

3 Results

The XRD spectra of vanadium doped alkaline earth lead zinc phosphate glass systems at different compositions is shown in Fig. 1. The XRD spectra inform no continuous or otherwise discrete sharp peaks, that indicate the characteristics of the amorphous nature of present glass system. Table 1 presents the different glass compositions prepared for the present investigation.

Figure 2 shows the optical absorption spectra of vanadium doped alkaline earth lead zinc phosphate glasses recorded at room temperature in the wavelength range 200-900 nm.

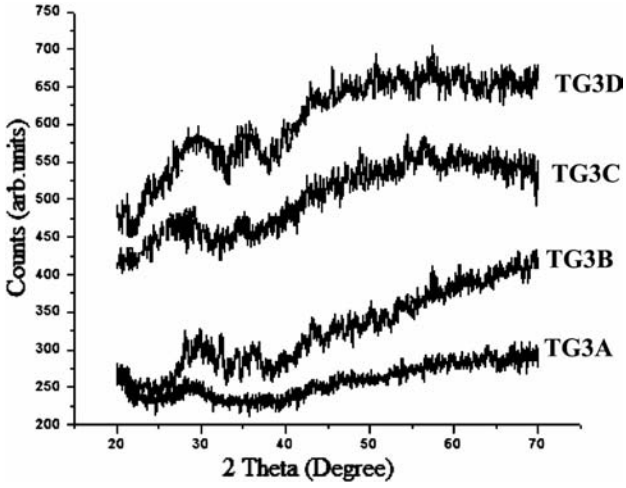

Fig. 1 — XRD graph of vanadium doped alkaline earth lead zinc phosphate glasses

Table 1—Glass composition (mole%)

Sample	Composition (mol %)
TG3A	59.9 P_2O_5-10 Pb_3O_4-10 ZnO-20 MgO-0.1 V_2O_5
TG3B	59.9 P_2O_5-10 Pb_3O_4-10 ZnO-20 CaO-0.1 V_2O_5
TG3C	59.9 P_2O_5-10 Pb_3O_4-10 ZnO-20 SrO-0.1 V_2O_5
TG3D	59.9 P_2O_5-10 Pb_3O_4-10 ZnO-20 BaO-0.1 V_2O_5

The optical basicity of an optical glass will reflect the ability of the glass to donate negative charge of the probe ion[13]. The theoretical values of the optical basicity of the glass are estimated by using the formula[14]:

$$\Lambda_{th} = \sum_{i=1}^{n} \frac{Z_i r_i}{2v_i}$$

where n is the total number of cations present, Z_i for the oxidation number of the ith cation, r_i for the ratio of the number of i_{th} cation to the number of oxides present and v_i for the basicity moderating parameter of the i_{th} cation. The basicity moderating parameter v_i is calculated from $v_i = 1.36\ (x_i - 0.26)$, where x_i is the Pauling electro negativity[15] of the cation.

Figure 3 shows the Tauc's plots of vanadium doped alkaline earth lead zinc phosphate glasses. The optical band gap energy in the amorphous system is closely related to the energy gap between the valence band and the conduction band[16,17]. In glasses, the conduction band is influenced by the glass forming

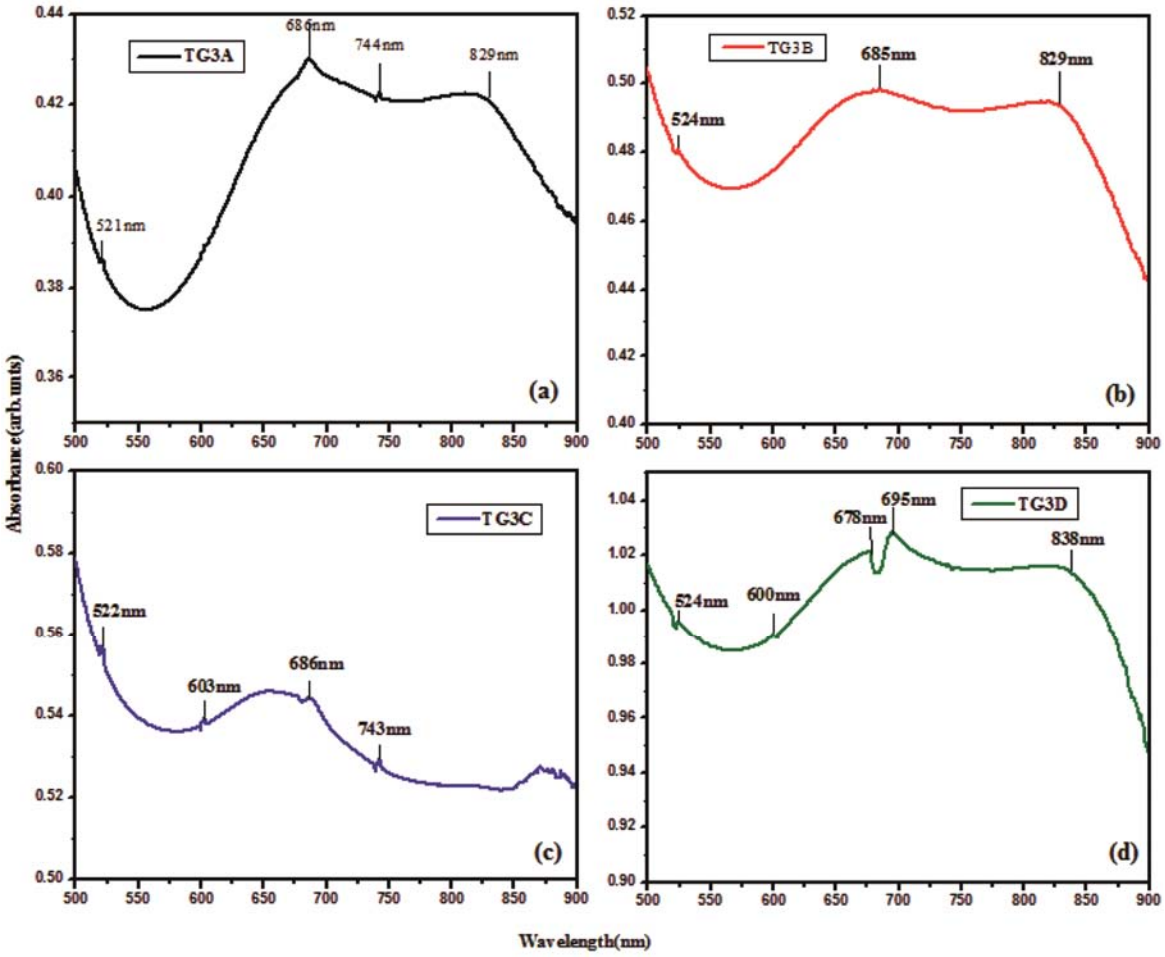

Fig.2 — Optical absorption spectra of vanadium doped alkaline earth lead zinc phosphate glasses

anions; the cations play an indirect but significant role[16]. The absorption edge study in the UV region being an useful method to understand the optical transition and electronic band structure in glasses, the direct and indirect optical transitions are calculated by following equation[18]:

$$\alpha(v) = \frac{\alpha_0[hv - E_{opy}]^n}{hv} \qquad \ldots(1)$$

where the exponent n = 1/2 for an allowed direct transition, while n = 2 for an allowed indirect transition, α_0 is a constant related to the extent of the band tailing, and E_{opt} the optical band gap energy. The absorption coefficient, $\alpha(v)$, is determined for nearing to the absorption edge of different photon energies for all glass samples. The values of optical band gap energy (E_{opt}) is determined from the plot $(\alpha hv)^{1/2}$

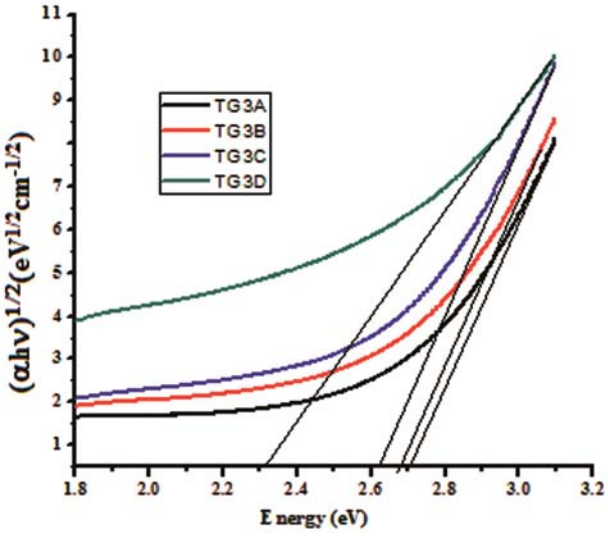

Fig. 3 — Tauc's plots of vanadium doped alkaline earth lead zinc phosphate glasses

versus photon energy (hv) (Tauc's plot), for allowed indirect transitions. The values of the optical band gap and the Urbach energies from Tauc's plots of the glasses are presented in Table 3.

The EPR spectra of the glass systems have structures that are characteristic of hyperfine interactions arising from an unpaired electron with ^{51}V nucleus, whose spin is 1/2 and present in 99.75% abundance,are shown in Fig. 4. These spectra are analyzed by assuming[19-21] that vanadium present as vanadyl ions in a ligand field of C_{4V} symmetry. The EPR spectra are analyzed by using an axial spin-Hamiltonian Equation (2). The solutions of the spin-Hamiltonian[22], for parallel and perpendicular hyperfine lines are given as:

$$H_s=\beta_0 g_{\|} B_z S_z+\beta_0 g_{\perp}(B_x S_x+B_y S_y)+A_{\|} S_z I_z+A_{\perp}(S_x I_x+S_x I_y) \quad \ldots(2)$$

where β_0 is the Bohr magneton, B_x, B_y, B_z are the components of the magnetic fields, S_x, S_y, S_z the components of the electron spin operators, I_x, I_y, I_z the components of the nucleus spin operators.

The spin-Hamiltonian parameters for various compositions are presented in Table 4. Fermi contact interaction term K, dipolar hyperfine coupling parameter P and the covalency rates $(1-\alpha^2)$ and $(1-\nu^2)$ are calculated according to the following equations[23] and are given in Table 5.

$$A_{\|}=-P[K-4/7-\Delta g_{\|}-3/7\Delta g_{\perp}] \quad \ldots(3)$$

$$A_{\perp}=-P[K-2/7-11/14\Delta g_{\perp}] \quad \ldots(4)$$

where $\Delta g_{\|}=g_{\|}-g_e$ and $\Delta g_{\perp}=g_{\perp}-g_e$

$$\Delta g_{\|}=\frac{4\lambda\alpha^2\beta'^2 g_e}{\Delta E_2} \quad \ldots(5)$$

$$\Delta g_{\perp}=\frac{\lambda\nu^2\beta'^2 g_e}{\Delta E_1} \quad \ldots(6)$$

Figure 5 shows the variation of $[(\Delta g_{\|})/\Delta g_{\perp})]$ for different compositions of alkaline earth. The parameter β'^2 is assumed to be unity for many oxide glasses[23] and $(1-\nu^2)$, $(1-\alpha^2)$ represent the covalency rates. The covalency rates are evaluated by taking ΔE_1 = 12500 cm^{-1} and ΔE_1 = 16000 cm^{-1} (Ref. 24) $(1-\alpha^2)$ that provide the estimation of the σ bonding with the equitorial ligands and the $(1-\nu^2)$ for an estimate of covalency of the Π bonding between the V^{4+} ion and the vanadyl oxygen.

The phosphate units (PO_4^{3-}) for phosphate glasses have existed in the range 400-1400 cm^{-1}. The phosphate ions in the p state have existed in tetrahedral symmetry showing four fundamental bonds viz., 1082 cm^{-1} (v_3), 980 cm^{-1} (v_1), 515 cm^{-1} (v_4) and 363 cm^{-1} (v_2). Here v_1 is non-degenerate, v_2=doubly degenerate, and v_3 and v_4 triply degenerate. In this case, v_3 and v_4 are infrared active. A typical infrared spectrum of vanadium doped alkaline earth lead zinc phosphate glasses is shown in Fig. 6. The Raman spectra (Fig. 7), facilitates to identify modes responsible for oscillations of well defined groups as *ortho*, *pyro* and *meta* phosphate groups.

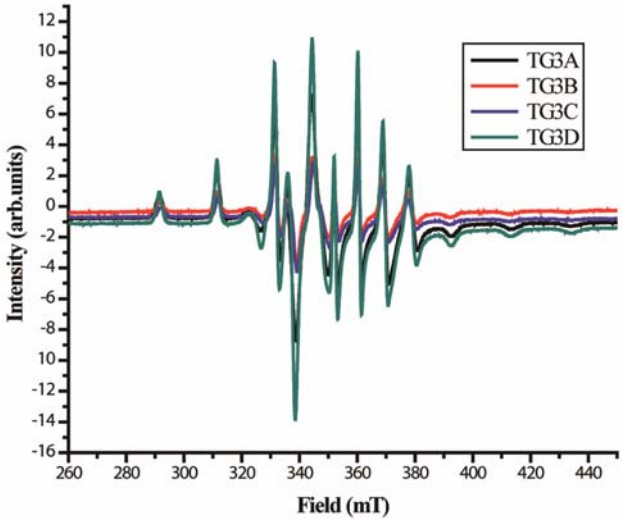

Fig. 4 — EPR spectra of vanadium doped alkaline earth lead zinc phosphate glasses

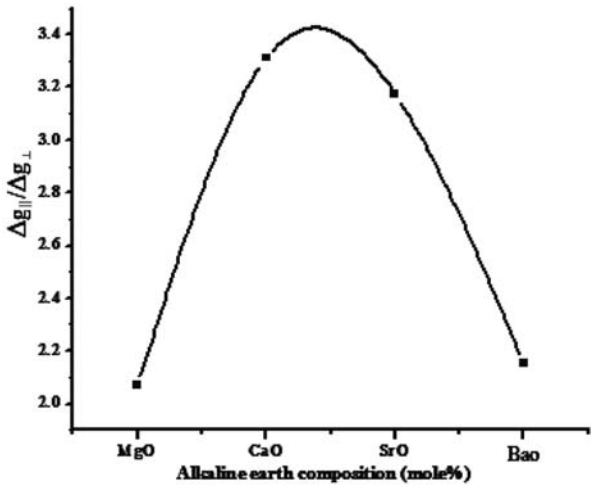

Fig. 5 — Variation of $[(\Delta g_{\|})/\Delta g_{\perp})]$ with alkaline earth composition

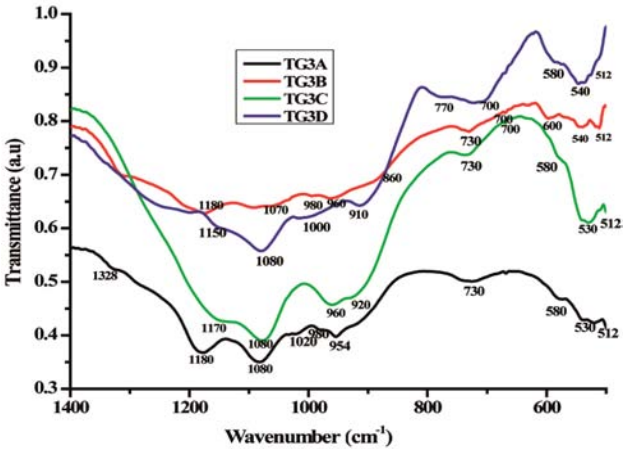

Fig. 6 — FT-IR spectra of vanadium doped alkaline earth lead zinc phosphate glasses

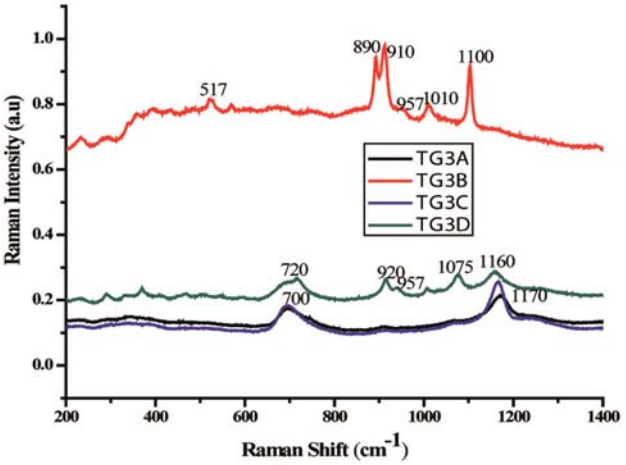

Fig. 7 — Raman spectra of vanadium doped alkaline earth lead zinc phosphate glasses

4 Discussion

The change in atomic geometrical configuration, coordination number, cross-link density and the dimensions of the interstitial space in the glass network will decide the density. Hence, the density is a tool in revealing the degree of change in the structure with the glass composition[25]. The increase in density is due to higher molecular weight of Pb_3O_4 compared to that of P_2O_5. The increase in density of the glass system indicates the change in the structure of the glass with replacement of alkaline earth content[26]. The data in Table 2 indicated that the average molecular weight increases from TG3A to TG3D glass which influences density, refractive index and other physical properties. The density and refractive index of TG3D glass is more, due to the addition of Ba^{2+} that provide ionic cross-linking between non bridging oxygen atoms and increase in the bond strength of this cross-link that is expected to improve chemical durability. The increase in refractive index is attributed to the generation of non-bridging oxygen (NBO) due to incorporation of V_2O_5 in the glass network. However, during the formation of glasses the orientation, arrangement and distribution of vanadium ions may differ in different glasses, which lead to different structural arrangements and bonding in glasses. This leads to differences in various physical properties.

Table 2 — Physical properties of vanadium doped alkaline earth lead zinc phosphate glasses

Physical Property	TG3A	TG3B	TG3C	TG3D
Refractive index (nd) at 589.3 nm	1.6385	1.6400	1.6405	1.6410
Density, d (gm/cm^3)	3.6512	3.6940	3.8670	3.9438
Average molecular weight, M (g)	169.903	173.118	182.626	192.568
Mean atomic volume (g/cm^3/atom)	8.4606	8.5084	8.5886	8.8778
Molar volume V_m (cm^3)	46.5334	47.3055	47.5267	48.8280
Field strength F ($\times 10^{15}$cm^{-2})	3.6577	3.6176	3.6218	3.4214

From Fig. 2, the optical spectra of all glasses in the present study have exhibited broad absorption bands in between 521 to 838 nm, corresponding to $^2B_{2g} \rightarrow {}^2B_{1g}$ to $^2B_{2g} \rightarrow {}^2E_g$ transition, a characteristic of VO^{2+} ions[27,28]. The assignment of these bands has been made on the basis of an energy level scheme for molecular orbitals of VO^{2+} ion in a ligand field of C_{4v} symmetry provided by Bullhausen and Gray[29]. The single d-electron of the VO^{2+} ion occupies the t_{2g} orbital in the octahedral crystal field and gives rise to $^2T_{2g}$ ground state. When excited, the electron occupies the upper e_g orbital and gives rise to ^2E_g term. In an ideal octahedral symmetry, only one band arising from the transition $^2T_{2g} \rightarrow {}^2E_g$ is expected. However, VO^{2+} has never exhibited an ideal octahedral symmetry but lowers to tetragonal (C_{4v}). In C_{4v} symmetry, $^2T_{2g}$ splits into $^2B_2$ and ^2E, whereas ^2E_g splits[23,29] into $^2B_1$ and $^2A_1$. The successive replacement of MgO by CaO, SrO and BaO has caused an increase in the peak height of these bands with a shift of peak position. Duffy and Ingram[14] reported that the ideal values of optical basicity can be predicted from the composition of the glass and the basicity moderating parameters of the various cations present. From

Table 3, it is found that the basicity parameter slightly increases from glass TG3A to TG3D. High optical basicity means high electron's donor's ability of the oxide ions to the cations. The optical band gap energy (E_{opt}) decreases whereas the values of Urbach energy (ΔE) increase with the successive replacement of alkaline earth content. The decrease in optical band gap and Urbach energy is attributed to the increase in non-bridging oxygen with the replacement of alkaline earth content.

The paramagnetism of the Vanadyl ion (V^{4+}) arises from a single unpaired electron, as the crystalline fields quench the orbital angular momentum. The crystal fields of V^{4+} ions in glasses can be described either by threefold or fourfold symmetries[30]. The variation of $g_{\|}$ and $g_{\perp}$ depends critically on the local symmetry of this field. Although the V^{4+} ions are usually in sixfold coordination in complexes containing vanadyl, its local symmetry is,generally, a distorted octahedron of oxygen ions. An octahedral site with tetragonal compression would give value[31] of $g_{\|}<g_{\perp}< g_e = 2.0023$ and $A_{\|}>A_{\perp}$.

From Table 4, it is observed that $g_{\|}< g_{\perp}$ and $A_{\|}> A_{\perp}$. It is confirmed that V^{4+} ions in the present glasses exist as VO^{2+} ions in octahedral coordination with tetragonal compression. The symmetry of vanadyl complex is C_{4v}, and the ground state of $3d^1$ ion is d_{xy}. The measure of tetragonality of the VO^{2+} site is given by $[(\Delta g_{\|})/\Delta g_{\perp})]$ values.

The present glass system containing (MgO, CaO, SrO and BaO), the $[(\Delta g_{\|})/\Delta g_{\perp})]$ values decrease in the order (CaO, SrO, BaO and MgO) as presented in Table 5. The decrease in the $[(\Delta g_{\|})/\Delta g_{\perp})]$ values suggests that the octahedral symmetry in these glasses is improved[32]. From Fig. 5, the variation of $[(\Delta g_{\|})/\Delta g_{\perp})]$ with different compositions of alkaline earth is non-linear which is perhaps due to change of ligand field in the transition metal (TM) ion site. In the present study, the values of $(1 - \nu^2)$ and $(1 - \alpha^2)$ indicate a moderate covalency for Π bonding and σ-bonding is significantly ionic. These values indicate only the trends in the variation of the magnitude of bonding parameters. Higher values of K indicate a large contribution to the hyperfine constant by the s electron. The hyperfine splitting for the glasses containing MgO, CaO, SrO and BaO is brought about by the increase of screening of the $3d_{xy}$ orbital from its nucleus through the overlap of the electron orbits of the surrounding ligands of oxygen[32].

The FT-IR spectra are composed of a number of overlapping absorption bands in the range 400-1400 cm^{-1}. The study of the structure of glasses is very important for the investigation of their properties. IR-transmitting glasses can be highly functional material in terms of the field structures. As can be seen in Fig. 6, absorption peak[33] around ~ 1328 cm^{-1} which can be assigned to P=O stretching vibration, in the branching group of Q^3 tetrahedral site is observed to exist in most phosphate glass system. The band at ~1177 cm^{-1} is due to the vibrations of PO_3^{2-} groups at the end of chains[34]. The bands around 1070 and 1080 cm^{-1} are assigned to the asymmetrical stretching vibration of P–O–P bond and stretching mode of Q^1 units [$\nu_{as}(PO_3^{2-})$], respectively[35]. Bands at 1020 and 1150 cm^{-1} are assigned to symmetric stretching vibration of PO_4^{3-}units in Q^0 species and symmetric stretching vibrations of PO_3^{2-} units in Q^1 species, respectively[36]. Another absorption peaks are located around 910-920 cm^{-1} are due to the stretching vibration [37]of P–O^-. The peaks at around 940–960 cm^{-1} are assigned to vibrations of P–O and phosphate groups[38]. A small absorption peak occur around 770 cm^{-1} is due to symmetric stretching modes of

Table 3 — Optical basicity (Λ_{th}), optical band gap (E_{opt}) and Urbach (ΔE) energies of vanadium doped alkaline earth lead zinc phosphate glasses

Samples	Optical basicity Λ_{th}	Optical band gap energy E_{opt} (eV)	Urbach energy ΔE (eV)
TG3A	0.4128	2.7084	0.1764
TG3B	0.4436	2.6768	0.2458
TG3C	0.4446	2.6231	0.2431
TG3D	0.4520	2.3198	0.2898

Table 4 — Spin-Hamiltonian parameters of vanadium doped alkaline earth lead zinc phosphate glasses

Sample	$g_{\|}$	$g_{\perp}$	$\Delta g_{\|}$	$\Delta g_{\perp}$	$A_{\|}$ (10^{-4} cm^{-1})	$A_{\perp}$ (10^{-4} cm^{-1})
TG3A	1.952	1.978	0.0503	0.0243	176.477	60.230
TG3B	1.948	1.986	0.0543	0.0163	182.095	61.021
TG3C	1.941	1.983	0.0613	0.0193	181.892	60.745
TG3D	1.950	1.978	0.0523	0.0243	182.921	61.667

Table 5 — Tetragonality and covalency rates of Vanadium doped alkaline earth lead zinc phosphate glasses

Sample	$[(\Delta g_{\|})/\Delta g_{\perp})]$	$(1 - \alpha^2)$	$(1 - \nu^2)$	K	P (10^{-4} cm^{-1})
TG3A	2.069	0.598	0.504	0.732	129.341
TG3B	3.312	0.566	0.667	0.729	133.693
TG3C	3.176	0.510	0.606	0.727	132.911
TG3D	2.152	0.582	0.504	0.724	134.625

P–O–P linkages, (P–O–P)s. The band at ~730 cm^{-1} is due to the stretching vibrations of oxygen atoms in P–O–P bridges. On the basis of previous reports, a band~ 700 cm^{-1} can be assigned to a covalent bond between non bridging oxygen and calcium, strontium ions as P–O–Ca, P–O–Sr stretching vibrations[39]. These glasses consist of pyrophosphate, Q^1 structure, based on bands at 1020 and 920 as well as the band at 730 cm^{-1} in FT-IR spectra.

The bands at ~532 cm^{-1} and 580 cm^{-1} correspond to the fundamental frequency of PO_4^{3-} in the Q^0 structure or harmonics of P-O-P and O=P-O bending vibrations[40]. The band at about 540 cm^{-1} is due to either harmonics of P-O-P bending vibration or to the characteristic frequency of $P_2O_7^{4-}$group[39,41]. The band at 517 cm^{-1} can be assigned both to angular deformation vibration of the O–V bond[42] or/and to the harmonics of bending vibration of O=P–O linkages[43]. The bands below 600 cm^{-1} are also ascribed to vibration of PbO, ZnO or any metallic cations such as Mg^{+2}, Ca^{+2}, Sr^{+2} and Ba^{+2} [44]. Thus, PbO, ZnO act as a network participant filled in the interspaces of PO_4 units in the form of Pb^{2+}, Zn^{2+} ions. This result suggests that alkaline earth oxides enter the glass network interstitially, as a network modifier; and it is known that when modifier cations are added to phosphate glasses depolymerization takes place through breaking linkages between Q^3 units and/or Q^3 and Q^2 units and increasing disorder of phosphate glass. On the other way, with the replacement of MgO/CaO/SrO/BaO content, the glass matrix leads to more P=O bonds breakage and may be to form the P–O–Mg/P–O–Ca/P-O-Sr/ P–O–Ba bonds[45].

The Raman spectra, like FTIR spectra in this work, have exhibited similar results as reported in earlier studies. Raman spectra indicate that addition of a modifying oxide to P_2O_5 network results in formation of non-bridging oxygen at the expense of bridging oxygen and this resulting depolymerization of phosphate network with the replacement of alkaline earth oxide explained by Brow[46]. The two main peaks observed at about ~700 cm^{-1} and ~1160 cm^{-1} are referred to symmetric stretching mode of P–O–P bridging bonds and to the symmetric stretching PO_2^-bonds on Q^2 tetrahedra[47].The shoulder at ~1075 cm^{-1} is related to symmetric PO_3 stretch on Q^1 tetrahedra and at ~1170 cm^{-1} is related to asymmetric stretching of PO_2 bonds, respectively[48]. A shoulder at ~720 cm^{-1} could be due to the second symmetric stretching mode of P-O-P bridging bonds in short phosphate units[49]. A band at 760 cm^{-1} is attributed to P–O–P bridging vibration in pyrophosphate groups[50]. A band at ~920 cm^{-1} band is assigned to the vibration in the $PO_2^-$and PO_3^-groups[51]. The higher peak of intensity at ~ 517 cm^{-1} can be assigned to phosphate bending motion P-O; at ~ 910 cm^{-1} to V-O stretching vibration modes, and at ~1100 cm^{-1} to $\nu_s(PO_2)^-$. Usually, bands observed between 957 cm^{-1} and 1100 cm^{-1} may be assigned to PO_4 stretch on Q^0 tetrahedra, PO_3 stretch on Q^1 tetrahedra, PO_2 stretch on Q^2 tetrahedra and P-O stretch on Q^3 tetrahedra, respectively.

The band at ~1010 cm^{-1} observed in the pyrophosphates is due to $P_2O_7^{4-}$ ions[52]. The intensity of the 1160 cm^{-1} band is caused by the PO_2 groups decrease and it becomes broader with the replacement of BaO with transition metal oxide content because of the depolymerization of the phosphate matrix and the increase of the disorder in glass. The bands below 600 cm^{-1} are related to network bending vibrations[53].

5 Conclusions

The optical absorption spectra exhibit an intense and broadband in the visible region and are related to VO^{2+} ions in a ligand field of C_{4v} symmetry. The optical band gap energy and the Urbach energy have been found to be dependent on the size of the alkaline ion. From EPR measurements, it is found that the vanadyl ions appear as isolated species in present glasses and occupied tetragonally compressed octahedral sites. The covalency rates ($1- \nu^2$) and ($1 - \alpha^2$) have represented a moderate covalency for Π-bonding, and the σ-bonding is significantly ionic. FT-IR spectra have indicated that phosphate network becomes more depolymerized and the amount of P=O bonds is reduced by the replacement of alkaline earth content. The Raman spectra have showed the breakage of P=O bond and the formation of P–O–P ones. The vibrations due to metallic cations (Mg^{2+}, Ca^{2+}, Sr^{2+} and Ba^{2+}) are also play an important role as a network modifier in their FTIR as well as Raman spectra.The replacement of BaO improves the strength of the cross-links between the phosphate chains of the TG3D glass.

Acknowledgement

The authors gratefully acknowledge UGC DRS LEVEL III program No. F.530/1/DRS/2009 (SAP-1), dated 9 February 2009, and DST FIST program No.

DST/FIST/PSI –002/2011 dated 20-12-2011, New Delhi, to the Department of Physics, ANU for providing financial assistance.

References

1 Kordes E E & Vogel W & Feterowsky R, *Z Elektrochem*, 57 (1953) 282.
2 Anantha P S & Hariharan K, *Mater Chem Phys*, 89 (2005) 428.
3 Nayab Rasool Sk, Rama Moorthy L, Jayasankar C K, *Solid State Sciences*, 22 (2013) 82.
4 Fathy M Ezzldin, *Indian J Pure & Appl Phys*, 43 (2005) 579.
5 Aref M Al-syadi, Sayed Yousef El, El-Desoky M M, & Al-Assiri M S, *Solid State Sciences*, 26 (2013) 72.
6 Stefan R, Simedru D, Popa A & Ardelean I, *J Mater Sci*, 47 (2012) 3746.
7 Wazer J R V, *J American Chemical Society*, 72 (1950) 647.
8 Acharya B S & Nayak B B, *Indian J Pure & Appl Phys*, 46 (2008) 866.
9 Muralidhara R S, Kesavulu C R, Rao J L, Anavekar R V & Chakradhar R P S, *J. Phys Chem Solids*, 71 (2010) 1651.
10 Galeener F L & Mikkelsen J C, *Solid State Commun*, 30 (1979) 505.
11 Hudgens J J & Martin S W, *J Am Ceram Soc*, 76 (1993) 1691.
12 Srinivasa Rao A, Rupa Venkateswara Rao B, Prasad M V V K S, Shanmukha Kumar J V, Jayasimhadri M, Rao J L & Chakradhar R P S, *Physica B*, 404 (2009) 3717.
13 Guedes de Sousa E, Mendiratta S K & Machado da Silva J M, *Portugal Phys*, 17 (1986) 203.
14 Duffy J A & Ingram M D, *J Inorg Nucl Chem*, 37 (1975) 1203.
15 Pauling L, *The Nature of Chemical Bond* (Cornell University Press, New York), 3rd Edn, 1960, p. 93.
16 Dayananad C, Sarma R V G K, Bikshmaiah G & Salagram M, *J Non-Cryst Solids*, 167 (1994) 122.
17 Fuxi G, *Optical and spectroscopic properties of Glass* (Germany-Berlin: Spinger), 1992, p.62.
18 Abdel-Baki M, El-Diasty F & Wahab F A A, *Optics Communications*, 261 (2006) 65.
19 Hochstrasser G, *Phys Chem Glasses*, 7 (1966) 178.
20 Seth V P, Yadav S & Gupta S K, *Radiat Eff & Defects Solids*, 132 (1994) 187.
21 Bogomolva L D & Jachkin V A, *J Non-Cryst Solids*, 58 (1983) 165.
22 McKnight J M, Whitmore K A, Bunton P H, Baker D B, Vennerberg D C & Feller S C, *J Non-Cryst Solids*, 356 (2010) 2268.
23 Kivelson D & Lee S K, *J Chem Phys*, 41 (1964) 1896.
24 Sreedhar B, Indira P, Bhatnagar A K & Kojima K, *J Non-Cryst Solids*, 167 (1994) 106.
25 Gaafar M S, Marzouk S Y & Mady H, *Philos Mag*, 89 (2009) 2213.
26 Shelby J E, *Introduction to glass science & technology* (Royal Society of Chemistry, Cambridge) 2nd Edn. 2005.
27 Fang S F & Bihui H, *Jin Sizho Bopuxue Zazhi*, 10 (1993) 9.
28 Ballhausen C J, *Introduction to Ligand Field Theory* (McGraw Hill, New York), 1962.
29 Ballhausen J & Gray H B, *Inorg Chem*, 1 (1962) 111.
30 Hecht H G & Johnston T S, *J Chem Phys*, 46 (1967) 23.
31 Abragam A & Bleaney B, *Electron Paramagnetic Resonance of Transition Metal Ions* (Oxford, Clarendon), 1970, p.175.
32 B&yopadhyay A K, *J Mater Science*, 16 (1981) 189.
33 Metwali E, Karabulut M, Sidebottom D L, Morsi M M, Brow R K, *J Non-Cryst Solids*, 344 (2004) 128.
34 Le Saout G, Simon P, Fayon F, Blin A, Villas Y, *J Raman Spectrosc*, 33 (2002) 740.
35 Arzeian J M & Hogarth C A, *J Mater Sci*, 26 (1991) 5353.
36 Dayan& C, Bhikshamaiah G, Jaya Tyagaraju V, Salagram M & Krishna Murthy A S R, *J Mater Sci*, 31 (1996) 1945.
37 Shih P Y, Yung S W & Chin T S, *J Non-Cryst Solids*, 244 (1999) 211.
38 Bhargava R N & Condrate R A, *Appl Spectrosc*, 31 (1977) 230.
39 Abo-Naf S M, El-Amiry M S & Abdel-Khalek A A, *Opt Mater*, 30 (2008) 900.
40 Aseem E E & Elmehasseb I, *J Mater Sci*, 46 (2011) 2071.
41 Rafiqul Ahsan Md & Golam Mortuza M, *J Non-Cryst Solids*, 351 (2005) 2333.
42 Saddeek YB, Shaaban ER, Aly KA & Sayed IM, *J Alloys Compd*, 478 (2009) 447.
43 Doweidar H, Moustafa YM, El-Egili K & Abbas I, *Vib Spectrosc*, 37 (2005) 91.
44 El-Egili K, *Physica B*, 325 (2003) 340.
45 Peng Y B & Day D E, *Glass Technol*, 32 (1984) 166.
46 Brow R K, *J Non-Cryst Solids*, 263/264 (2000) 1.
47 Liu H S, Shih P Y & Chin T S, *Phys Chem Glasses*, 38 (1997) 123.
48 Le Saout G, Fayon F, Bessada C, Simon P, Blin A & Vaills Y, *J Non-Cryst Solids,* 293 &295 (2001) 657.
49 El Hezzat M, Et-tabirou M, Montagne L, Bekaert E, Palavit G, Mazzah A & Dhamelincourt P, *Mater Lett*, 58 (2003) 60.
50 Hubert T, Mosel G & Witke K, *Phys Chem Glasses,* 27 (2001) 114.
51 Garbarczyk J E, Machowski P, Wasiucionek M, Tykarski L, Bacewicz R & Aleksiejuk A, *Solid State Ionics*, 136 (2000) 1077.
52 de Waal D & Hutter C, *Mat Res Bull,* 29 (1994) 1129.
53 Šantic A, Moguš-Milankovic A Furic K, Bermanec V, Kim C W & Day D E, *J Non-Cryst Solids,* 353 (2007*)* 1070.